IMWA 2025 Portugal Spain

Application of X-Ray-Tomography and Geochemical Modeling to Optimize AMD Treatment Design Using DAS at a former Tin Mine Site in France

K. Rhino, J. Jacob, A. Lassin, F. Duré, J. Engevin, J. Huron, V. Guérin

BRGM, 3 av. Claude-Guillemin – BP 36009 – 45060 ORLÉANS Cedex

Abstract

First pilot-scale trials of Dispersed Alkaline Substrate (DAS) reactors for treating acid mine drainage (AMD) at a closed Sn mine in Abbaretz, France revealed notable iron precipitation and clogging over time (Jacob et al., 2023). To address this, a fixed-bed limestone reactor was used to estimate precipitate volume via X-ray tomography, linking iron precipitation to porosity reduction. A second DAS reactor (with new condition) was conducted and a geochemical model, developed with PHREEQC, was used to simulate calcite dissolution, AMD neutralization, and iron hydroxide precipitation under varying residence times. DAS results aligned with experimental data, offered insights into DAS efficiency and lifespan, and helped identifying the main mechanisms that control the fate of iron and metals at the different stages of the process. These findings inform the design of robust passive treatment systems for long-term AMD management.

Keywords: Acid mine drainage, DAS, geochemical modelling, iron precipitation, Clogging

Introduction

AMD poses a substantial environmental challenge due to its high acidity and metal and metalloid content, which can contaminate water resources. DAS reactors offer a promising passive treatment solution by neutralizing acidity and facilitating metal precipitation through calcite dissolution (Ayora *et al.*, 2013). Compared to classical anoxic limestone bed, DAS can handle to an extent passivation/clogging due to ferric iron and aluminum thanks to inert wood chips. However, over time iron precipitation can still lead to clogging, limiting system efficiency and lifespan. Understanding the interplay between residence time, precipitate formation, and porosity evolution is critical for optimizing DAS reactor performance. This study combines laboratory experiments and X-ray tomography to estimate molar volume of precipitate, providing insights to enhance the design and long-term viability of AMD treatment systems.

Methods

Iron precipitate investigations

A 0.25 L fixed-bed limestone reactor was used to simulate AMD treatment (neutralization and iron precipitation). The downflow glass column (diameter 4.5 cm, total height 46 cm) contained 390 g of limestone (500 µm–4 mm particles) with a 262 mL bed volume and 40.8% porosity. A synthetic AMD (pH 2.45, 75 mg/L of Fe(III)) was pumped at 55 mL/h for 72 h, then at 28 mL/h for 53 h. Outlet pH was monitored every 5 minutes. Inlet and outlet samples were collected at 9, 24, 30 and 95 h, filtered (0.45µm) and acidified. Dissolved Fe and Ca were quantified by Agilent 4210 MP-AES. Setup photo is in supplementary material S1. A 6 mm-thick water layer coated the limestone bed. Residence time was about 2h in the column.

Following this experiment, the first 55 mm of the limestone column were scanned in an

X-ray microtomograph (ULTRATOM from RX-solutions (Chavanod, France)) with a 28.4 µm voxel size. Scanning parameters were 120 kV (voltage) and 200 µA (tube current) with a 1 mm Al filter. ImageJ software (Schneider *et al.*, 2012) and voxel counter plugin were used to calculate porosity and precipitate volume based on X-ray absorption differences among air, limestone and precipitate.

The apparent molar volume of the precipitates was estimated using the measured volume from computer tomography (CT) scans and the amount of iron precipitated, acknowledging that the precipitates consist of iron oxyhydroxides with an uncertain exact composition, hydration state, nature of the mineral and according to the following equation:

$$apparent\ molar\ volume\ = \frac{Volume\ of\ AMD\ treated\ \times ([Fe_{in}] - [Fe_{out}])}{Volume\ of\ precipitates}$$

Where Fe_{in} and Fe_{out} are inlet and outlet Fe dissolved molar concentration.

DAS reactor

A 60 cm high square column (30 cm × 30 cm) was filled with calcite (17% vol. grain size 0–4 mm) and wood (83% vol. grain size 0–30 mm). The average composition of the water in the inlet was pH = 2.75, 206 mg/L of Fe, 19 mg/L of Ca and 18 mg/L of Al. The output effluent was on average pH = 6.4, 86 mg/L of Fe, 290 mg/L of Ca and 0.1 mg/L of Al. The residence time in the DAS is 30 h. A 5 cm-thick water film coated the limestone bed.

Modelling of DAS reactor

Geochemical modelling was performed using the PHREEQC code (Parkhurst and Appelo, 2013) in conjunction with a modified version of the Thermoddem database (Blanc *et al.*, 2012). This database decouples Fe(II) and Fe(III) redox valencies, allowing for detailed simulation of non-equilibrium redox-sensitive processes. The model was designed to simulate the injection of AMD into a DAS reactor. The primary objectives were to predict iron depletion at the column outlet, evaluate changes in porosity over time, and simulate the neutralization of acidity within the column.

The column was divided into five cells. The first cell contained a 5 cm water layer in equilibrium with the atmosphere, with a porosity of 100%. The remaining cells represented layers filled with calcite (wood was not specifically modelled, because considered inert), with a total porosity of 54%. An average AMD composition was used for modelling despite natural variations. Hydrological parameters were calibrated using a conductivity residence time test with low conductivity water, later replaced by AMD. The model simulated acid neutralisation, iron redox reactions, and mineral process. The first cell modelled Fe(II) oxidation to Fe(III) by oxygen using Singer and Stumm (1970) rate law. Calcite dissolution and acid neutralization reactions followed rate laws derived from Marty *et al.* (2015). Precipitation processes included only ferrihydrite ($Fe(OH)_3$) and gibbsite ($Al(OH)_3$), as the main precipitation process occurring in the column

The model calibration used experimental data collected during the first 50 days of the experiment, during which the DAS was operational without notable issue including clogging.

Results

Iron precipitate investigations

The fixed-bed limestone reactor presented good performances throughout the duration of the experiment with effluent pH increasing from 2.5 to 6.7, Ca concentration increasing from 61 to 341 mg/L and Fe concentration decreasing from 75 to less than 5 mg/L (detection limit). After 72 hours, a rise in the water level in the column caused by an increase in pressure drop was observed, it was probably due to a decrease in porosity of the fixed-bed. The AMD flow rate was then halved to avoid an overflow during the next 53 hours. By the end of the experiment, the water level rose from 6 mm to 28 mm above the limestone.

Fig. 1 (obtained with X-ray Computational microtomography, CT) overlays the evolution of porosity and precipitates (expressed as a percentage of the total area of each horizontal slice) with depth on a vertical CT slice of the column. Precipitates are highlighted in red. Image processing did not allow for a clear distinction between the precipitates and

the interface of the limestone grains. This was accounted for in the calculation of the percentage and volume of precipitates by subtracting a baseline measurement taken at the bottom of the column (between 45 and 55 mm from the top). Minimum porosity was found at between 10 and 15 mm depth (approximately 26%), then gradually increased downwards to about 37.9% near the base of the column, a value close to the pre-neutralization porosity (40.8%). No effect of carbonate dissolution was observed (due to limited operation time and the uncertainty of the measurements). The precipitates were most concentrated at the top of the column, where the iron-laden AMD entered, occupying a maximum of approximately 20% of the column volume. The slice with the most precipitates is shown in supplementary material S2. This proportion steadily decreased toward the bottom, becoming nearly negligible after 35 mm. Interestingly, the minimum porosity occurred approximately 10 mm below the maximum precipitate concentration, likely due to the irregular surface of the limestone packing.

The apparent molar volume of the precipitates was calculated as 825 cm^3/molFe. Assuming the precipitate is primarily ferrihydrite (given the near-neutral pH conditions), this value was compared to the molar volume of ferrihydrite (reported in the Thermoddem database, Fe(OH)3: 34.36 cm^3/mol). The calculated in-situ value was 24 times higher, reflecting the loose nature of the undried precipitate in place within the reactor. This 1:24 ratio (or ≈4%) is consistent with the typical solid content of iron sludge found in passive mine water settling ponds (Zinck *et al.* 1997). This highlights the consequence of the low density of the precipitate and absence of structure on the operational performance and lifespan of the treatment system as pressure drop became measurable after only 3 days of experimentation. This confirms the importance of wood chips in the DAS mixture for maintaining open porosity.

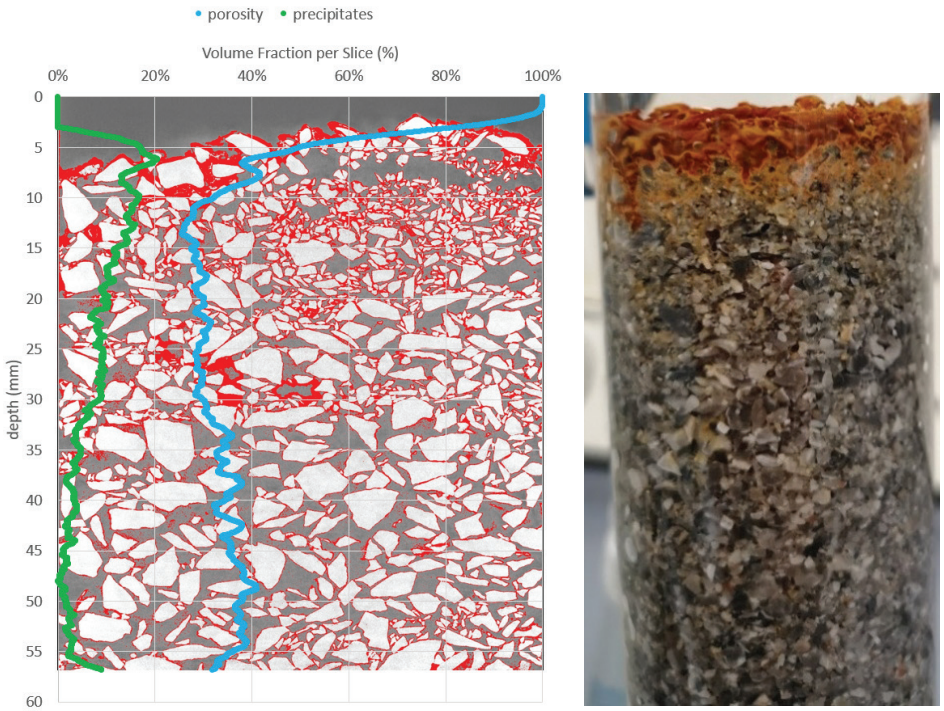

Figure 1 *On the left, evolution of porosity and precipitates (expressed as a percentage of the total area of each horizontal slice) with depth on a vertical CT slice of the middle of the column. In red the iron precipitate, and in white and grey limestone grains and porosity respectively; on the right, photo of the top of the column by the end of the experience.*

Modelling of DAS reactor

The hydrodynamic parameters required for modelling were established using an electrical conductivity test. The initial total porosity is 54%, hydraulic conductivity is estimated to 2×10^{-6} cm/s, and the dispersivity was 0.01 m.

Simulations for residence times of 24, 30 (experimental residence time), 36, and 48 hours revealed key insights into iron depletion, pH evolution, and mineral precipitation (Fig. 2). Overall, the simulations showed that the overall column reached a steady reactivity after 5 days of experimentation, suggesting that the interaction between the AMD effluent and the DAS is the result of a chemical equilibrium. Iron retention increased with longer residence times: for example, 24-hour simulations showed 55% retention, while 48-hour simulations showed 65%. The simulation for the experimental residence time (30 hours) matched the observed data well (58% of iron retention). The pH evolution was consistent across residence times, driven by the kinetic dissolution of calcite with a simulated final pH of 6.8 compared to the experimental pH of 6.4 (30 h residence time). This difference may result from local variations in chemical composition or edge effects, the square

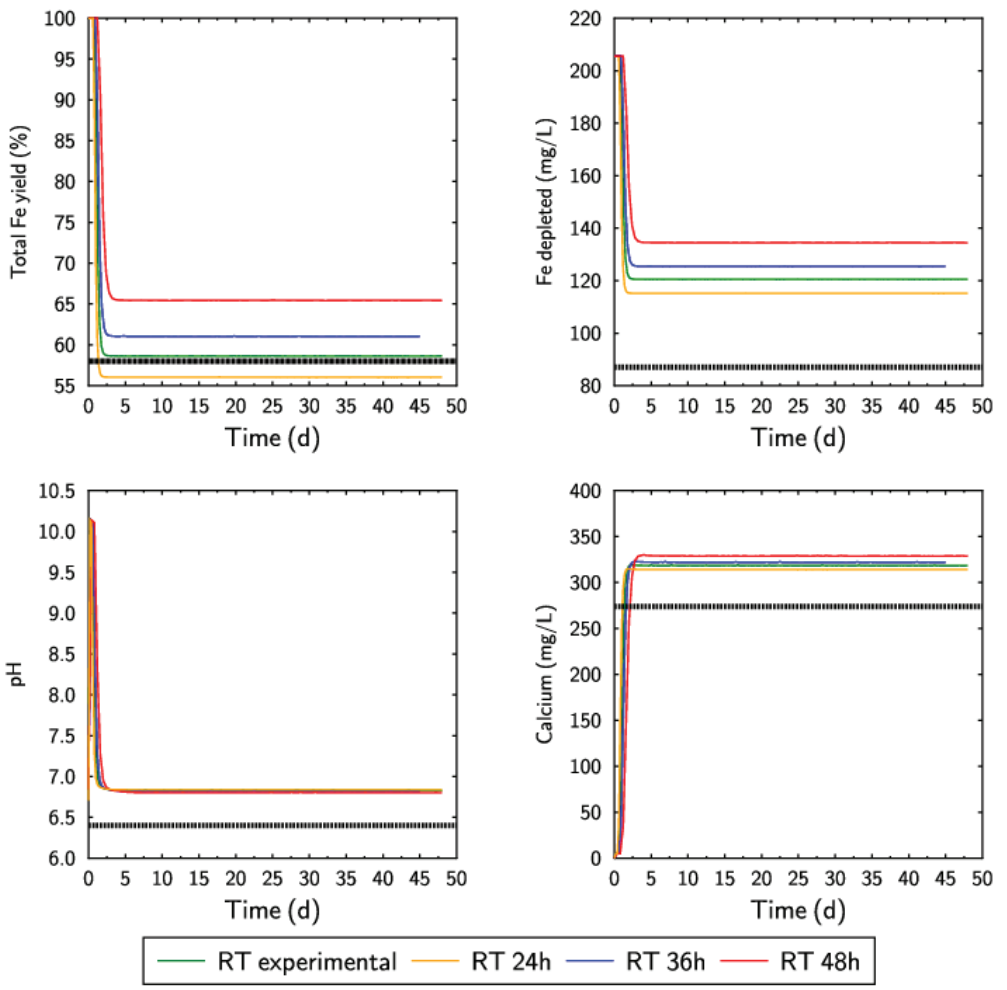

Figure 2 *Simulation of the evolution of the Total Fe yield, Fe depletion, pH and calcium concentration as a function of residence time. Black dashed lines represent the experimental value after 50 days of experimentation. Green, yellow, blue and red lines represent the results for respectively the experimental residence time (30 hours), and residence time of 24, 36 and 48 hours.*

reactor shape may allow a portion of the injecting solution to bypass reactions with calcite. Mixing the final output solution with 5–10% of unreacted AMD gave a pH of 6.5 approaching the experimental pH of 6.4. Iron precipitation trends aligned with iron retention: the 24-hour simulation exhibited 120 mg/L of iron removal from the injected AMD, while the 48-hour simulation showed 140 mg/L of iron removal. These simulated values were higher than the experimental result of 85 mg/L Fe removed from the injected water. Accounting for 5–10% AMD bypass at the reactor edges brought simulated values closer to experimental data.

Calcium concentration is similar across all simulations with a final value fluctuating around 325 mg/L whereas experimental data shows a final value of 275 mg/L in the effluent. This gap in Ca concentration can be attributed to the edge effect which limits the dissolution of calcite in the edges. This result aligns with the pH findings which reveal that less dissolved calcium leads to a more acidic final pH or calcite specific surface area was different in the experiment.

The volume mass of the in situ undried precipitates estimated by X-ray microtomography (825 cm^3/mol Fe) was incorporated into the simulation to assess porosity changes over time. This was performed instead of considering the mass density of each mineral precipitating and dissolving into the system. While this kind of calculation in PHREEQC is typically used for diffusion-dominated processes, here the simulation was adapted to estimate porosity changes across the DAS under flow conditions. However, it is important to note that the simulations did not account for the feedback effect of porosity reduction on flow rates, meaning that decreased porosity did not lead to a simulated decreased residence time in the layer.

The simulation results showed that shorter residence times considerably accelerated porosity reduction (Fig. 3), attributable to a greater flow of fresh AMD, leading to increased dissolution of calcite. This apparent contradiction with calcium and iron concentration in the effluent can be explained by the higher influx of dissolved iron with a shorter residence time. For instance, with a residence time of 24 hours, the iron influx was 147 mg/h, with 55% (80.8 mg/h) depleted at the outlet. Conversely, at a 48-hour residence time, the influx was 84 mg/h, with 65% (54.6 mg/h) depleted. Despite the higher depletion efficiency at longer residence times, the greater absolute iron precipitation in the shorter residence time scenario led to faster porosity decline due to increased

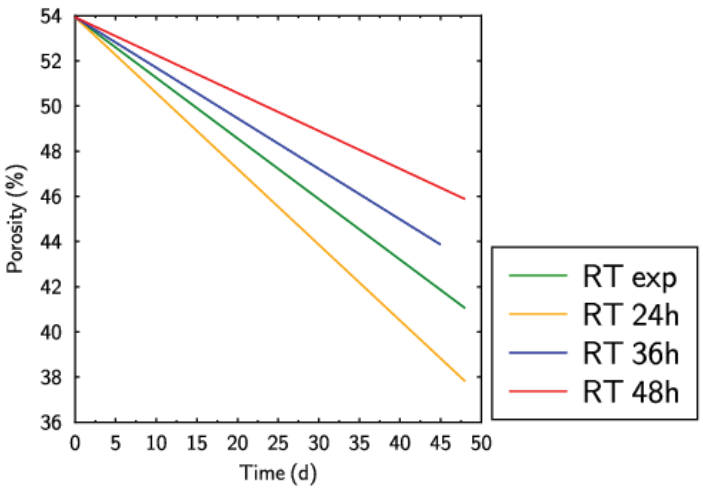

Figure 3 *Evolution of porosity as a function of residence time. Experimental results show a final porosity of 48%. Green, yellow, blue and red lines represent the results for respectively the experimental residence time (30 hours), and residence time of 24, 36 and 48 hours.*

precipitate formation within the DAS reactor. Considering the experimental final measured porosity was about 48% after functioning for 100 days, Fig. 3 shows that the simulations (50 days) overestimates the porosity change. The model does not consider the edge effect or the passivation of the grain which could slow down the overall decrease of porosity. Although the code has its limitations, it provides a useful approximation of porosity changes and highlights the critical role of residence time in DAS performance.

Conclusions

This study underscores the importance of residence time and iron precipitation on DAS reactor performance for AMD treatment. Laboratory experiment and X-ray microtomography revealed porosity reduction due to precipitate build up, while reactive transport modeling captured key geochemical processes. Shorter residence times could accelerate clogging and increase porosity decline, emphasizing the need for careful optimization of operational parameters. Furthermore, these insights enable a better-informed choice between smaller, less costly reactors with shorter lifespans, which require more frequent replacement of the packing material, and larger, more expensive reactors designed to last longer due to slower clogging rates. By quantifying precipitate volume and porosity effects, this study offers practical guidance for enhancing DAS reactor efficiency and ensuring sustainable AMD treatment.

Acknowledgements

The authors would like to thank the DPSM for funding and supporting this research. We also extend our gratitude to the MIMAROC platform of BRGM for providing access to the X-ray microtomography facilities used in this study. We thank Stephane Gaboreau for the µ-tomography acquisition.

References

Jacob J, Moreau U, Duré F, Engevin J, Huron J, Lassin A, Guérin V (2023, July). AMD passive treatment using DAS at an old tin mine in France. In IMWA 2023.

Ayora C, Caraballo MA, Macias F, *et al* (2013) Acid mine drainage in the Iberian Pyrite Belt: 2. Lessons learned from recent passive remediation experiences. Environ Sci Pollut Res 20:7837–7853. https://doi.org/10.1007/s11356-013-1479-2

Schneider CA, Rasband WS, Eliceiri KW (2012) NIH Image to ImageJ: 25 years of image analysis. Nat Methods 9:671–675. https://doi.org/10.1038/nmeth.2089

Parkhurst D.L., Appelo C.A.J. (2013) Description of input and examples for PHREEQC version 3: a computer program for speciation, batch-reaction, one-dimensional transport, and inverse geochemical calculations (No. 6-A43), U.S. Geological Survey, Techniques and Methods. Reston, VA.

Blanc Ph, Lassin A, Piantone P, *et al* (2012) Thermoddem: A geochemical database focused on low temperature water/rock interactions and waste materials. Applied Geochemistry 27:2107–2116. https://doi.org/10.1016/j.apgeochem.2012.06.002

Marty NCM, Claret F, Lassin A, *et al* (2015) A database of dissolution and precipitation rates for clay-rocks minerals. Applied Geochemistry 55:108–118. https://doi.org/10.1016/j.apgeochem.2014.10.012

Singer PC, Stumm W (1970) Acidic Mine Drainage: The Rate-Determining Step. Science 167:1121–1123. https://doi.org/10.1126/science.167.3921.1121

Zinck JM, Wilson JL, Chen TT, Griffith W, Mikhail S, Turcotte AM (1997, May) *Characterization and stability of acid mine drainage treatment sludges*; MEND Report 3.42.2a; Natural Resources Canada (CANMET): Ottawa, Ontario, Canada, 73 pp.